Measurements-based Power Control - A Cross-layered Framework

Berk Birand, Howard Wang, Keren Bergman, Gil Zussman

Department of Electrical Engineering, Columbia University, New York, NY 10027

{*berk,howard,bergman,gil*}*@ee.columbia.edu*

Abstract: Despite the emergence of dynamic optical devices, operational networks are still mostly static. To enable future dynamic operation, we present a cross-layered optimization framework that adapts the wavelengths' power levels based on real-time OPM measurements.

OCIS codes: (060.4250) Networks, (060.4256) Networks, network optimization.

1. Introduction

The emergence of dynamic optical devices has the potential to allow network reconfigurability based on traffic and Quality-of-Transmission (QoT) requirements. However, *core networks are still largely static* due to the unpredictable effects of impairments [1]. As a result, most lightpaths are usually not modified once assigned and most of the changes are executed manually, which is both time-consuming and expensive [2]. Optical Performance Monitors (OPMs) that measure QoT values in real-time will be one of the enablers for reconfigurable networks [3]. However, most control schemes that use OPMs operate at the link scale rather than at the network scale [3]. A promising paradigm for using OPM measurements at the network scale is cross-layering [4, 5, 6].

In this paper, we propose and evaluate a *cross-layered framework for wavelength power control*. We formulate a network-scale problem whose solution yields feasible lightpath power and attenuation levels while satisfying QoT constraints (regarding BER and OSNR). The problem formulation takes into account the impairments caused by the interactions between different lightpaths. The problem has to be solved when changes take place in the network (e.g., addition or removal of lightpaths), and therefore, the framework can facilitate the dynamic operation of higher layer algorithms, such as Routing and Wavelength Assignment (RWA). The unique properties of the framework stem from the fact that the analytic functions related to the problem (e.g., BER functions) are not explicitly known. Yet, observations regarding the convexity of the various functions allow us to develop an algorithm that is based on OPM measurements. The algorithm not only converges to the solution based on noisy measurements and without explicit knowledge of the functions, but also aims to do so with a small number of OPM activations.

2. Problem Formulation and Algorithm

Fig. 1(a) illustrates the dynamics of a fiber span within an optical link. Each wavelength λ_i on span u is associated with a power level p_i^u. This power is reduced by fiber loss α^u, amplified by G_i^u, and attenuated by D_i^u (all in dB). Hence, for the downstream span v, $p_i^v = p_i^u - \alpha^u + G_i^u - D_i^u$. We assume that the launch power at the first span (p_i^u) and the amplification level (G_i^u) are controlled variables and that the rest are constants. OPMs at the end of a span can measure the BER and OSNR on different wavelengths. The measured BER and OSNR values for λ_i on span u depend on p_i^u and G_i^u as well as the power levels of all other wavelengths on that span. Hence, we denote the measurement readings from the OPMs by the *performance functions* $\mathrm{BER}_i^u(p)$ and $\mathrm{OSNR}_i^u(p)$, where p refers to the vector of all power levels in the network (p depends on G, the vector of amplification levels).

Based on the network capabilities and the SLAs, operators may need to solve various power control problems. A specific example referred to as the *Performance Guarantee* (PG) Problem is shown in Fig. 1(b).[1] The solution to the

[1] Versions of the problem with objective functions related to power consumption or QoT can be solved by similar algorithms to the one described.

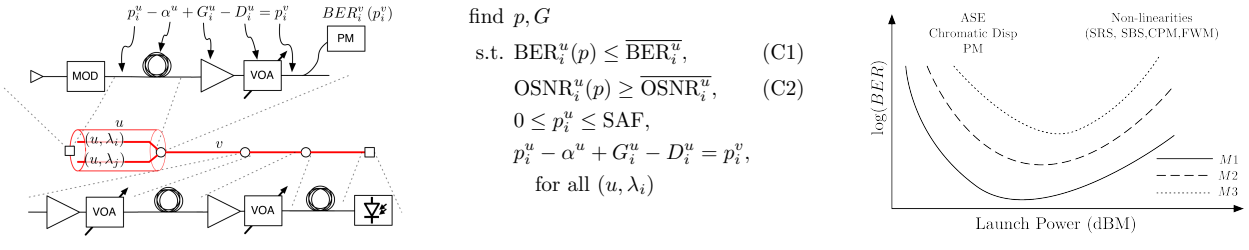

(a) (b) (c)

Fig. 1: (a) A link composed of several spans and the corresponding link model; (b) the PG Problem whose objective is to find a feasible power assignment satisfying the BER and OSNR constraints; and (c) illustration of the BER as a function of the optical launch power for a few modulation schemes ($M1$, $M2$, and $M3$) [7, 8]. In each region, the most prominent impairments are marked.

PG Problem includes feasible vectors of power (p) and amplification (G) levels such that the BER and OSNR at the OPMs satisfy constraints (C1) and (C2)[2]. A solution framework for the PG Problem enables the dynamic addition of lightpaths. Specifically, when a new lightpath has to be added (e.g., as determined by an RWA algorithm), additional constraints have to be added to the PG Problem for the new lightpath (the constraints for the existing lightpaths have to be maintained) and some of the performance functions may change. Then, the algorithm has to converge to a feasible solution for the PG Problem under the new constraints. A similar process has to take place when a lightpath is removed.

At first glance, the PG Problem seems to be intractable. Yet, it is known that $\mathrm{BER}_i^u(p)$ is convex in p_i^u and that $\mathrm{OSNR}_i^u(p)$ is concave in p_i^u [7, 8]. As an example, Fig. 1(c) illustrates $\mathrm{BER}_i^u(p)$ as a function of p_i^u.[3] To the best of our knowledge, the relationship between $\mathrm{BER}_i^u(p)$ and the power levels $p_j^u,\ j \neq i$ have not been thoroughly characterized. Hence, in the following section *we experimentally show that* $\mathrm{BER}_i^u(p)$ *is convex in* p_j^u by plotting in Fig. 2(c) the BER function over a range of attenuation levels. The cuts along the x- or y-axes of this function yield convex curves similar to Fig. 1(c). However, this does not not imply that the *multidimensional* function is convex over *both* variables, which we establish graphically and by calculating the Hessian. Similar relationships also hold for OSNR_i^u. Due to these observations, *the PG Problem is a convex program*, and hence, has a well-defined solution.

While the PG Problem is a convex program, it has special characteristics that pose significant challenges. First, many convex optimization algorithms require the functions' derivatives in order to find a descent direction. However, the analytical expressions for the performance functions ($\mathrm{BER}_i^u(p)$, $\mathrm{OSNR}_i^u(p)$) and their derivatives are unknown, and therefore, such methods are inapplicable. Another alternative is to use the OPMs to estimate the derivatives by computing differences. Yet, this does not yield acceptable results, due to relatively large measurement errors. Finally, each evaluation of the functions not only requires readjusting the power levels in the network but can also be expensive in terms of power and time as it requires access to the OPM device.

We propose an algorithm, referred to as the Performance Guarantee Solver (PGS), that tackles the challenges outlined above and solves the PG Problem efficiently. PGS is based on a coordinate search algorithm that does not require derivatives. Instead, given a set of directions that span the entire variable space, it gradually improves the solution. By selecting an application-specific set of directions that are most likely to yield improvement, PGS minimizes the number of OPM measurements required for convergence. A log-barrier objective function $\phi_\mu(p)$ incorporates the OPM measurements $\mathrm{BER}_i^u(p), \mathrm{OSNR}_i^u(p)$ and is defined as: $\phi_\mu(p) = \sum_{(u,\lambda_i)\in\mathscr{V}} s_i^u - 1/\mu \sum_{(u,\lambda_i)} \left[\log\left(\overline{\mathrm{BER}_i^u} - \mathrm{BER}_i^u(p) + s_i^u\right) + \log\left(\mathrm{OSNR}_i^u(p) - \overline{\mathrm{OSNR}_i^u} + s_i^u\right) \right]$, where s_i^u are the *slack variables* for the set of violated constraints $\mathscr{V}$ and $\mu \geq 0$ is a parameter. The $\log(\cdot)$ operation is well-defined when the measurements satisfy constraints (C1) and (C2). For constraints that are not satisfied, the introduction of a positive slack variable achieves feasibility. As $\mu \to \infty$, the relative weight of the logarithms is reduced and PGS prioritizes decreasing the slack variables to make the problem feasible. Therefore, the objective of PGS is $\min \phi_\mu(p)$ as $\mu \to \infty$, namely to minimize the slack variables s_i^u until the constraints (C1) and (C2) are satisfied.

Due to the use of the log-barrier function, a constraint that is satisfied will never be violated. Namely, if an intermediate step of PGS violates a constraint, the logarithm function will guarantee that this iteration will be discarded. Since the framework operates on a live network, such a guarantee is important. Also note that while optimization problems are usually solved offline during the network planning phase, PGS is supposed to run continuously during the network operation, and if the constraints and functions change (e.g., when adding a lightpath) it converges to a new solution.

3. Simulation and Experimental Results

We evaluated the performance PGS analytically, via simulation, and experimentally (the analytical performance evaluation is out of scope). We focus on performance evaluation in the context of network restoration. Specifically, we consider a scenario in which following a fiber cut, a wavelength has to be added to another fiber. We assume that the replacement wavelength is determined by an RWA algorithm and is not already provisioned. PGS has to accommodate the change by adjusting the power levels in real-time on all the necessary spans.

Our experimental setup is shown in Fig. 2. Eight CW DFB laser sources evenly spaced from C36 to C43 on the 100 GHz ITU grid are evenly partitioned into two wavebands (Λ_{long} and Λ_{short}). Each waveband is multiplexed onto a single fiber and fed into a variable optical attenuator (VOA) in order to provide fine-tuned control of its injected power. The outputs of each VOA are then multiplexed together, modulated by a $LiNbO_3$ Mach-Zehnder modulator (MOD) driven with a 10 Gb/s NRZ-OOK $2^{15}-1$ PRBS pattern originating from a pulse pattern generator (PPG), and decorrelated by approximately 10 km of SMF-28 fiber.

[2] In general, a subset of constraints (C1) and (C2) have to be included, based on the OPMs' availability at different locations.

[3] The exact shapes of the functions depend on the modulation scheme, and the fiber, amplifier, and other equipment characteristics [7, 8].

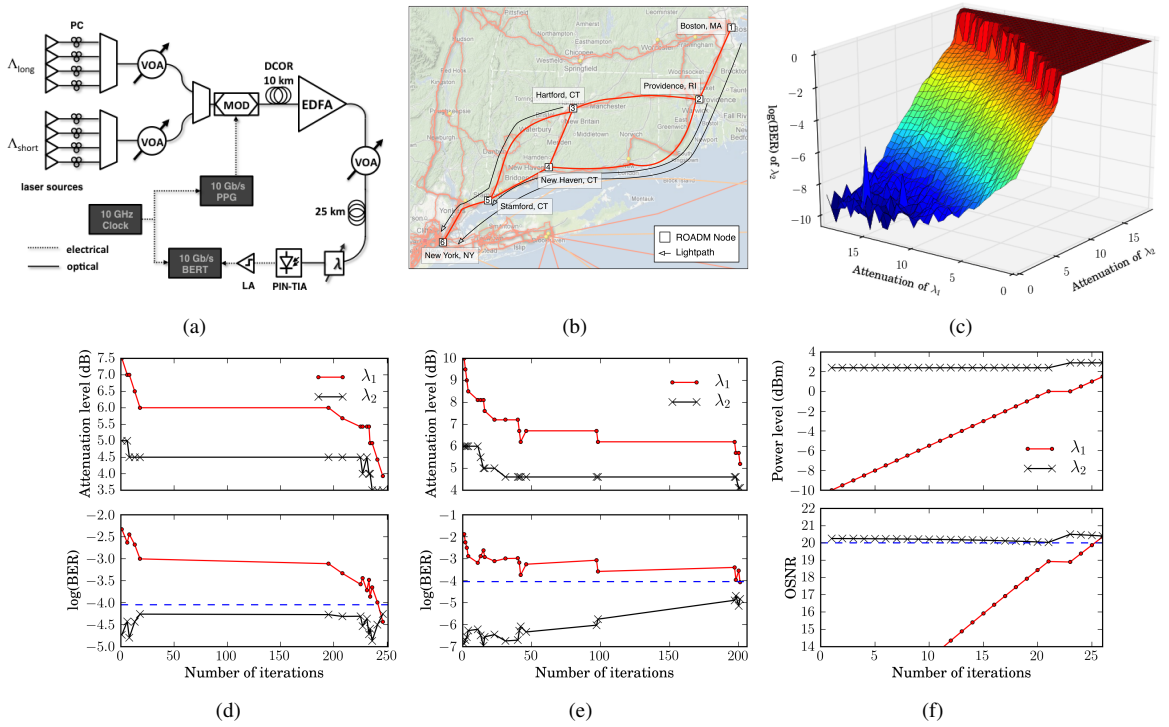

Fig. 2: (a) A schematic of the experimental setup; (b) part of the Level 3 network, used in the simulation experiments; (c) the experimentally obtained 3-dimensional function that demonstrates the convexity of the BER curve of λ_2 with respect to the attenuation levels of λ_1 and λ_2. (d,e,f) the evolution of the attenuation and BER levels in two testbed experiments and a simulation experiment.

Inter-channel impairments are induced through a segment consisting of an EDFA, VOA, and 25 km of SMF-28. The EDFA is tuned to operate in saturation within a subrange of the operating powers of the incident wavebands. As a result, at significantly high powers, each waveband will "steal gain" from the other, resulting in a mutually-degraded signal. Due to the high sensitivity of the receiver, the VOA serves to attenuate the signal to just within the limits of its dynamic range. Representative channels from each waveband (C39 and C40) are isolated using a tunable filter (λ) and received by a PIN-TIA coupled to an inline limiting amplifier (LA). The electronic signal is then evaluated on a bit-error-rate tester (BERT), the results from which are used as the real-time performance metric for feeding into PGS.

In order to evaluate the performance of the PGS algorithm in an automated manner, we interface a PC with the VOAs, tunable optical filter, and BERT via the IEEE-488 GPIB interface. Through this interface the algorithm collects measurements from each data stream and iteratively modifies the attenuation level of each waveband.

First, as mentioned above, we used the testbed to validate the convexity assumption (see Fig. 2(c)). Then, we conducted extensive experiments in which wavelength λ_2 is active and λ_1 is being added. For two experiments, the evolution over time of the power levels (as determined by PGS) and the BER measurements of both wavelengths are shown in Figs. 2(d) and 2(e). In Fig. 2(d), the BER of λ_2 is close to the threshold indicated by the dashed line. While the power of λ_1 is increased, the power of λ_2 is also increased in order to stay under the threshold. In Fig. 2(e), the BER of λ_2 is initially significantly below the threshold. When λ_1 is added, the power level of λ_2 is increased so that its BER is closer to the threshold, avoiding unnecessary power expenditure. Note that wavelength addition takes approximately 200 OPM evaluations and does not require manual intervention.

Finally, we conducted simulation experiments for similar restoration scenarios. We used the ATOM simulator developed at Bell Labs [9] and considered part of the Level 3 network illustrated in Fig. 2(b). In this 6-node network, 90 lightpaths are transmitting between various cities at 2 dBm. We consider a case where wavelength λ_1 is added between Boston and New York and the effects are measured on wavelength λ_2 between Hartford, CT and New York. The resulting dynamics are shown in Fig. 2(f). As can be seen, when the power of λ_1 is increased, the OSNR on λ_2 hits its threshold and the power of λ_2 is increased.

References

[1] S. Woodward *et al.*, in "OECC'10," (2010).
[2] R. Doverspike *et al.*, Proc. IEEE **100**, 1092 –1104 (2012).
[3] Z. Pan *et al.*, Optical Fiber Technology **16**, 20–45 (2010).
[4] J. Sole-Pareta *et al.*, Proc. IEEE **100**, 1118 –1129 (2012).
[5] C. Lai *et al.*, in "PHO Annual 2010," (2010).
[6] S. Azodolmolky *et al.*, Comput. Netw. **53**, 926 – 944 (2009).
[7] A. Gnauck, in "IEEE/LEOS Annual Meeting," (2004).
[8] M. S. Islam *et al.*, J. Opt. Netw. **6**, 295–303 (2007).
[9] C. Chekuri *et al.*, Bell Labs Tech. J. **11**, 129–243 (2006).

This work was partially supported by NSF grant CNS-1018379 and CIAN NSF ERC under grant EEC-0812072.